

Multi-twist retarders for broadband polarization transformation

Ravi K. Komanduri, Jihwan Kim, Kristopher F. Lawler, and Michael J. Escuti

North Carolina State Univ, Dept Electrical & Computer Engineering, Raleigh, NC (USA)

ABSTRACT

We introduce a family of broadband retarders, comprised of a low number of twisted nematic liquid crystal layers, that accomplishes well-controlled polarization transformation for nearly any bandwidth desired. For example, we show that broadband linear to circular polarization conversion can be achieved with only two twist layers where the performance matches the popular three-waveplate approach by Pancharatnam. Using liquid crystal polymers on a single substrate, we show how these multi-twist retarders are embodied as a monolithic birefringent plate with excellent performance and potentially very low cost.

Keywords: achromatic, broadband, twist, quarter-wave, chiral, liquid crystal

1. INTRODUCTION

Polarization transformation is important to many optical devices, including, but not limited to, Liquid Crystal Displays (LCDs), optical storage (e.g., CD/DVD/Blu-ray Disc), 3D movie cinemas, optical remote sensing, and optical fiber networks. This is distinctly different from the topic of broadband linear and circular polarizers¹ where the goal is to create light of a specific polarization from unpolarized light by reflecting, redirecting, or absorbing the unwanted light. Generally polarization converters are used in combination with these polarizers to transform the polarization state of light to a desired output, depending on the application. Common examples of polarization converters include quarter-wave and half-wave retardation elements,² which can be used to transform linear to circular and linear to a different linear polarization, respectively, or vice versa. In many of these applications, broadband or achromatic polarization conversion may be required across a desired spectral range, as in the case of 3D movie goggles and transfective LCDs operating in the visible wavelength region.

Narrowband polarization converters are also referred to as waveplates or phase retarders, and are often created by using optically birefringent materials. Although form birefringence³ in isotropic materials can be used to achieve the same function, we limit our discussion to materials with uniaxial optical birefringence, including but not limited to birefringent crystals, stretched polymer films, and liquid crystal layers. Traditionally, achromatic retarders were created by stacking waveplates formed from different inorganic materials⁴ such as Calcium Fluoride, Magnesium Fluoride, Quartz etc. By arranging stacks of these materials with opposing optical axes and carefully chosen thicknesses, broadband operation is achieved by appropriately balancing the difference in the dispersion of the material birefringence. Since this approach depends on the availability of natural minerals or grown crystals, the size and cost of these elements is prohibitive in many cases, among other limitations related to performance. This principle has been applied to both stretched polymer films,^{4,5} and LC cells⁶ to create achromatic retarders. However the use of multiple materials is often undesirable because of increased sensitivity to variations in incident angle, and temperature.

An alternative approach is to use two or more discrete waveplates, typically formed of the same material, wherein their optical axis orientations and individual retardations are not usually orthogonal or otherwise trivial, as discovered by Pancharatnam.⁷ The simplest case involves just three waveplates, but this can be extended to various combinations. While these can be formed with nearly all the conveniently available birefringent films mentioned for narrowband waveplates, including LCs, each discrete waveplate must be formed on its own as a physically separate element and subsequently aligned with extreme precision to the other elements. This requirement adds substantially to fabrication cost, often leads to thick (i.e., many mm or cm) components, and also results in a constrained angular aperture, among other limitations.

Correspondence should be addressed to: mjescuti@ncsu.edu, +1 919 513 7363

An additional category of broadband polarization transforming elements consists of single inhomogeneous birefringent layers, almost always formed with uniaxially birefringent materials that have a local optical axis that is not uniform throughout the thickness. These have long been used in LCDs⁸ and other optical devices. Most commonly, they form the addressable layer, as in the case of 90° twisted nematic (TN) and super-twisted nematic (STN)⁹ LCDs, but such films have also been used as compensation films with positive and negative birefringence. While these act as polarization transformation elements, often with some achromatic behavior, they have severe limitations on what input and output polarizations may be transformed. For example, 90°-TN and STN birefringent layers only transform linear to near-linear polarizations, and most compensation films make only small adjustments to the polarization.

In a few cases, combinations of twisted layers have also been used for broadband polarization transformation.^{10,11} A broadband quarter-wave retarder was demonstrated by using two twisted nematic cells fabricated separately, and subsequently aligned.¹² In all of these cases, the elements are disclosed as being formed separately and subsequently aligned with each other. We demonstrated broadband polarization gratings¹³ to achieve achromatic diffraction over the visible range. This represents a particular monolithic design where two self-aligned LC layers are used, that have the same thickness but opposing twist angles. Here we extend the central concept to achieve broadband polarization conversion, by analyzing stacks of twisted LC layers using Jones Calculus. We realize that a whole new family of Multi-Twist Retarders (MTRs) exists, that are easy to fabricate, requiring just one alignment layer which can be created in rubbed polymers or photo-alignment materials. We demonstrate achromatic QWPs formed as MTRs for the visible range, using just two LC layers, that rival the performance of all conventional designs discussed. These devices can be easily tuned for a wide range of wavelengths without sacrificing performance, and for various LC materials. The simplicity of these designs makes them robust, and extremely viable for volume manufacturing. As a result, patterned MTRs are already being used as one of the key components in a new generation of Polarization Conversion Systems (PCS)¹⁴ for portable projectors.

2. BACKGROUND

Jones Calculus² is often used to analyze the effect of LC layers on the polarization state of light. This simple approach is an effective way to study LC devices for small incident angles. More complicated models using extended Jones Matrices, or the Berreman 4 X 4 descriptions can be used to simulate the effect on the viewing angle of these elements, which are beyond the scope of this work. In the simplest case, polarized light can be easily represented by a two-dimensional Jones Vector \mathbf{J} which is given by Eq. 1. Here E_x and E_y are complex numbers that satisfy the relationship $|E_x|^2 + |E_y|^2 = 1$. Next we attempt to model birefringent twist layers using Jones Matrices.

$$\mathbf{J} = \begin{pmatrix} E_x \\ E_y \end{pmatrix} \quad (1)$$

2.1 Jones Representation of Birefringent Twist Layers

Several analytical expressions have been derived for analyzing LC twist layers accurately. Consider Fig. 1 which illustrates a generic twist layer that is completely characterized by three parameters: ϕ_1 , ϕ_2 , and d . $\Gamma = \pi\Delta n d/\lambda$ is the normalized retardation where Δn is the birefringence, d is the layer thickness, and λ is the wavelength of light. In the coordinate system shown, ϕ_1 and ϕ_2 are the optic axis orientations at the start and the end of the LC twist layer. The Jones Matrix T of this LC layer² is given by Eq. 2.

$$T = \begin{pmatrix} a - ic \cos \theta & -b - ic \sin \theta \\ b - ic \sin \theta & a + ic \cos \theta \end{pmatrix} \quad (2)$$

Here $\theta = \phi_1 + \phi_2$ while the coefficients in the above equation are given by Eqs. 3 where $\phi = \phi_2 - \phi_1$ represents the net twist angle of the LC layer, and $\text{sinc}X = \sin X/X$.

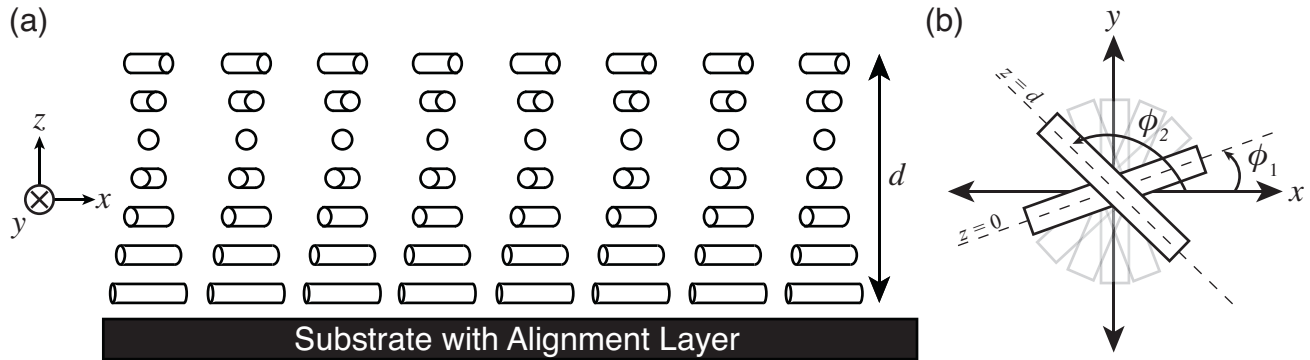


Figure 1. (a) Illustration of a general LC twist layer showing the continuous variation of the optic axis through the thickness. (b) Top-down view of the optic axis twist in the azimuthal plane.

$$\begin{aligned}
 a &= \cos X \cos \phi + \text{sinc} X (\phi \sin \phi) \\
 b &= \cos X \sin \phi - \text{sinc} X (\phi \cos \phi) \\
 c &= \Gamma \text{sinc} X \\
 X &= \sqrt{\Gamma^2 + \phi^2}
 \end{aligned} \tag{3}$$

In the above equations, a, b, c are purely real, and they satisfy the relation $a^2 + b^2 + c^2 = 1$. In the next section, we discuss how this simple representation can be used to analyze MTRs for a specific case.

2.2 MTR Design Process

Stacks of LC twist layers can be easily analyzed using Jones Matrices described in the previous section, for various kinds of polarization conversion. As an example, we describe how this approach can be used for converting linear to circular polarization states over a desired broadband range. Let \mathbf{J}_i and \mathbf{J}_o represent the Jones Vectors of the input and output respectively. They are related to each other by Eq. 4, where N twist layers are assumed.

$$\mathbf{J}_o = \left(\prod_{i=1}^N T_i \right) \mathbf{J}_i \tag{4}$$

Here \mathbf{J}_o can be expressed by Eq. 1. We now introduce the term ellipticity e , given by Eq. 5 in order to analyze linear to circular polarization converters. S_3 is the normalized Stokes parameter that is a measure of the amount of circular polarization, and is calculated using Eq. 6. Here E_x^* is the complex conjugate of E_x , and $Im(x)$ represents the imaginary part of the entity x . Note that e is real and can assume any value depending on the polarization state of light. For circularly polarized light, $e = \pm 1$ depending upon the handedness. Ellipticity is generally more sensitive to variations in the polarization state than the Stokes parameters, which could also be considered for this analysis.

$$e = \tan \left(\frac{\sin^{-1}(-S_3)}{2} \right) \tag{5}$$

$$S_3 = 2Im(E_x E_y^*) \tag{6}$$

The designs in the following sections were obtained by choosing a particular input polarization, usually along the horizontal or vertical directions. In this work, we deal with the specific case of achieving linear to circular polarization conversion for the visible wavelength range of 450-650 nm. The individual twist layer parameters were identified by running this optimization over a wide range of twist angles and thicknesses, with the constraint that the optic axis orientation varies continuously throughout the MTR structure. Similar approaches can be used to target other output polarizations as well.

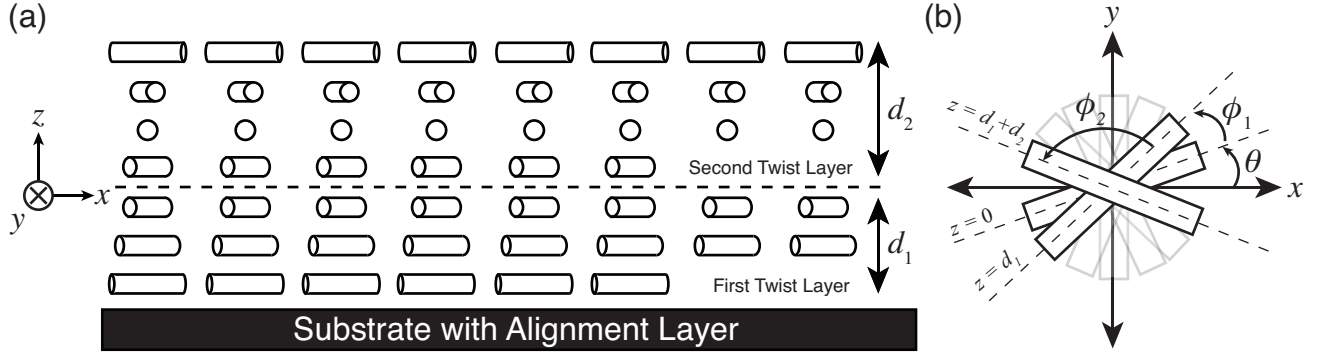


Figure 2. (a) Two-twist LC structure showing the individual layers. (b) Top-down view of the twist in optic axis in the azimuthal plane.

3. LINEAR TO CIRCULAR POLARIZATION CONVERTERS

Achromatic Quarter-Wave Plates (QWPs), that convert linearly polarized light into circular polarizations, are commonly used to create circular polarizers which are used in LCDs to block out ambient light, and to separate the constituent polarizations in 3D glasses. Here we try to analyze a generic two-twist LC structure, as shown in Fig. 2, to achieve this same functionality. The LC optic axis is assumed to vary continuously throughout this stack. Let θ represent the starting optic axis orientation of the first twist layer in the coordinate system shown. The nematic director twists through a first angle ϕ_1 over a thickness d_1 . The second twist layer then causes the director to twist through a second twist angle ϕ_2 over thickness d_2 . These five parameters sufficiently describe this two-twist structure within the framework of Jones Calculus, which we will now use for further analysis.

3.1 Jones Analysis

We assume that the input to the first twist layer is perfectly horizontally polarized. The output electric field is given by

$$\mathbf{J}_o = (T_2 T_1) \mathbf{J}_i = \begin{pmatrix} a_2 - ic_2 \cos \theta_2 & -b_2 - ic_2 \sin \theta_2 \\ b_2 - ic_2 \sin \theta_2 & a_2 + ic_2 \cos \theta_2 \end{pmatrix} \begin{pmatrix} a_1 - ic_1 \cos \theta_1 & -b_1 - ic_1 \sin \theta_1 \\ b_1 - ic_1 \sin \theta_1 & a_1 + ic_1 \cos \theta_1 \end{pmatrix} \begin{pmatrix} 1 \\ 0 \end{pmatrix} \quad (7)$$

Here $\theta_1 = 2\theta + \phi_1$ and $\theta_2 = 2\theta + 2\phi_1 + \phi_2$. The output electric field components are given by the following equations.

$$E_x = [a_1 a_2 - b_1 b_2 - c_1 c_2 \cos(\theta_2 - \theta_1)] - i [c_2(a_1 \cos \theta_2 + b_1 \sin \theta_2) + c_1(a_2 \cos \theta_1 - b_2 \sin \theta_1)] \quad (8)$$

$$E_y = [a_1 b_2 + a_2 b_1 - c_1 c_2 \sin(\theta_2 - \theta_1)] - i [c_2(a_1 \sin \theta_2 - b_1 \cos \theta_2) + c_1(a_2 \sin \theta_1 + b_2 \cos \theta_1)] \quad (9)$$

Here $a_i, b_i, c_i (i = 1, 2, 3)$ are the corresponding coefficients for the two twist layers. The Stokes parameter S_3 is reduced to the form in Eq. 10.

$$S_3 = 2c_2(a_1^2 - b_1^2)(a_2 \sin \theta_2 - b_2 \cos \theta_2) + 2c_1(a_2^2 + b_2^2 - c_2^2)(a_1 \sin \theta_1 - b_1 \cos \theta_1) - 4a_1 b_1 c_2(a_2 \cos \theta_2 + b_2 \sin \theta_2) - 2c_2 c_1^2(a_2 \sin(2\theta_1 - \theta_2) + b_2 \cos(2\theta_1 - \theta_2)) \quad (10)$$

The ellipticity e is then calculated by Eq. 5, which simplifies the optimization process significantly. For designing achromatic QWPs, the goal is to obtain nearly perfect circularly polarized light for the visible wavelength range of 450-650 nm. For Left Circular output, the optimization criterion is set to minimize the term $|e - 1|$ for the same wavelength range. Using this condition, we ran a series of simulations by varying the twist parameters for both layers. Next we discuss some of these solutions and compare their performance to that from conventional designs.

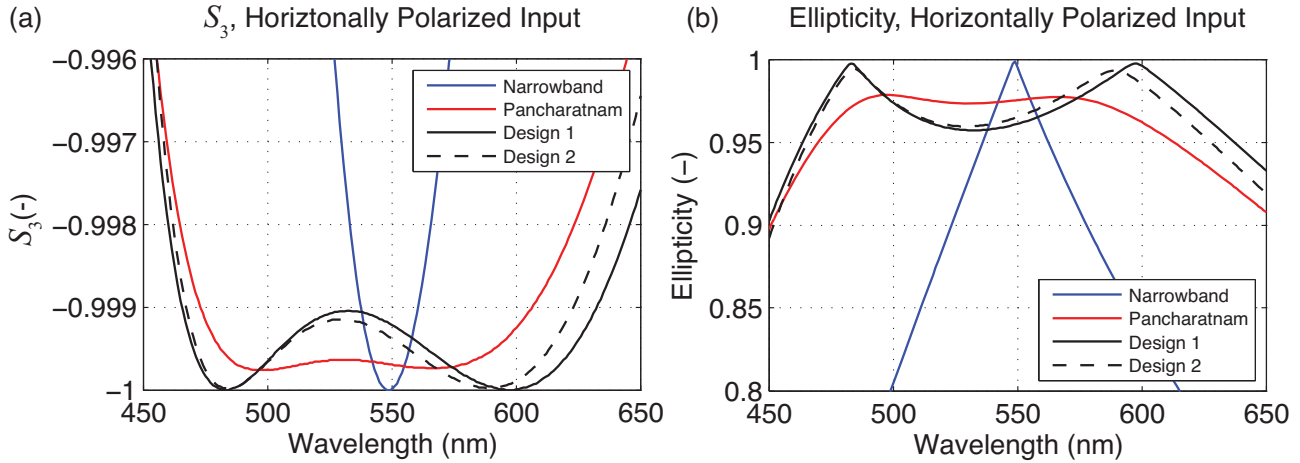


Figure 3. Comparison of (a) Stokes Parameter S_3 , and (B) Ellipticity e values for conventional and two-twist designs, calculated using Jones Calculus.

3.2 Calculation of Output Ellipticity

Here we attempt to calculate the performance of achromatic QWPs obtained by combinations of just two-twist layers modeled in the previous section. We assume a realistic dispersion in the LC birefringence given by Eq. 11 where λ is measured in nm. A uniformly aligned waveplate at 45° can convert horizontally polarized light into circularly polarized light at a single wavelength. As a baseline, consider a narrowband QWP that is $0.88 \mu\text{m}$ thick, which acts like a perfect QWP at 550 nm.

$$\Delta n = 0.128 + 8390/\lambda^2 \quad (11)$$

Using the same dispersion, a conventional achromatic QWP can be designed for the visible range as proposed by Pancharatnam. In the simplest arrangement, this is achieved by stacking three narrowband waveplates aligned at specific angles with respect to each other. For comparison purposes, we have calculated the waveplate parameters for this design using a similar optimization process, assuming the same LC birefringence as above. In this broadband QWP the first and last waveplates are identical, each with a thickness of $1 \mu\text{m}$, and an orientation angle of 79.6° respectively. The center waveplate has a thickness of $1.645 \mu\text{m}$, and an orientation angle of 10.7° .

DESIGN NO.	$\theta(^{\circ})$	$d_1(\mu\text{m})$	$\phi_1(^{\circ})$	$d_2(\mu\text{m})$	$\phi_2(^{\circ})$
1	5.0	1.600	18.0	1.000	80.0
2	58.7	0.830	29.9	1.365	-92.0

Table 1. Summary of design parameters for two-twist QWP structure.

Using the process described in the last section, design parameters for a two-twist QWP were calculated. These values are summarized in Table 1. Design 1 uses two twist layers that have opposite handedness while Design 2 consists of layers of same handedness. Note that there are several other combinations of twist angles, thicknesses, and start angles, that achieve a similar broadband performance in the visible range. The ones chosen in Table 1 represent a family of such designs with the smallest twist angles, best suited for fabrication.

Fig. 3 compares the performance of all the waveplates discussed in this section. Part (a) shows the S_3 parameter. The chromatic nature of the narrowband waveplates can be easily seen here where perfect operation, $S_3 = -1$ is achieved at precisely one wavelength. The broadband designs however are able to perform over a much larger wavelength range. Note the scale in part (a) which seems to suggest almost perfect performance over the entire range. The ellipticity on the other hand, plotted in part (b) amplifies the differences between the

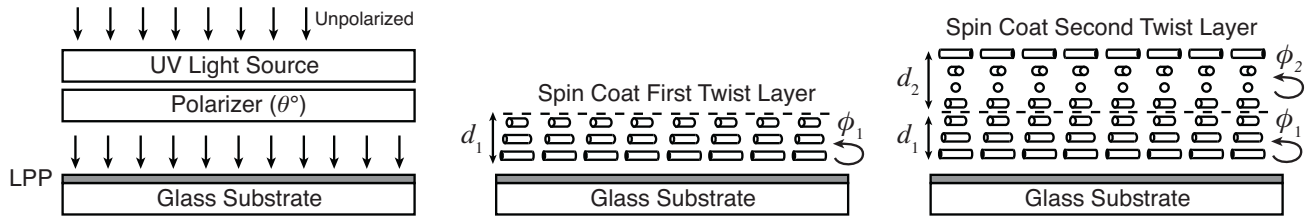


Figure 4. A brief summary of the two-twist QWP fabrication process.

different designs, because it is much more sensitive to small changes. Regardless, we can see that both the two-twist designs operate very well, and provide good achromatic performance that is comparable to the conventional design. Table 2 shows the average values for S_3 , and ellipticity which also reiterates this observation.

DESIGN TYPE	$\langle S_3 \rangle$	$\langle e \rangle$
Narrowband	-0.9722	0.8225
Pancharatnam	-0.9988	0.9590
Two-twist Design 1	-0.9993	0.9676
Two-twist Design 2	-0.9991	0.9648

Table 2. Average S_3 and ellipticity of output polarization calculated for the different designs over the visible range of 450-650 nm.

We note that the exact wavelength range over which the broadband QWP operation is achieved is dependent on the dispersion of birefringence given by Eq. 11. When we look at the design parameters in Table 1, the two-twist parameters are asymmetric for both the layers. Due to this, it is important that the LC twist layers are arranged specifically in the order discussed so far to achieve the correct polarization transformation, which is unlike conventional chromatic waveplates.

4. MTR FABRICATION

Broadband QWPs created as MTRs, not only represent the simplest arrangement of elements to achieve good performance for a wide range of wavelengths, but also present the easiest way to fabricate such elements. We have experimentally fabricated achromatic QWPs on glass substrates by spin coating just three polymer layers. This process is illustrated in Fig. 4. A photo-alignment material is first spin coat onto a glass substrate, and is patterned by using a polarized light source at the required orientation angle indicated in Table 1. Alternatively rubbed polyimide and other alignment materials can also be considered as viable options. We used solutions of Liquid Crystal Polymers (LCP) doped with chiral materials in a pre-determined ratio to create our twist layers in order to match the parameters in Table 1. The first twist layer is spin-coated directly on top of the alignment material using these mixtures, and is fully polymerized using a UV light source as shown in part (b). Finally the second twist layer is coated on top of this first layer, and is polymerized once again to complete the twist structure in part (c).

For the results presented in this work, we used the photo-alignment material LIA-CO01 (DIC Japan, Ltd) and exposed thin layers of this material using a broadband UV LED light source (Exposure energy of 2 J/cm^2 at 365 nm). A reasonable quality UV polarizer (Edmund Optics Ltd.) mounted appropriately was used to create linearly polarized light at the corresponding angle. The twist layers were created using the reactive mesogen prepolymer mixture RMS10-025, with $\Delta n \sim 0.16$ at 589 nm. Its dispersion is similar to Eq. 11 in the visible spectrum. In addition, chiral materials CB-15 (right-handed) and MLC-6247 (left-handed) were mixed in appropriate quantities to achieve broadband operation over the visible range. Design 1 only required the former while Design 2 required both the materials. The LCP layers were fully polymerized using the same UV exposure parameters as used for the LPP material. All RMS, CB and MLC aforementioned materials were obtained from Merck Chemicals Ltd. (i.e., EMD Chemicals).

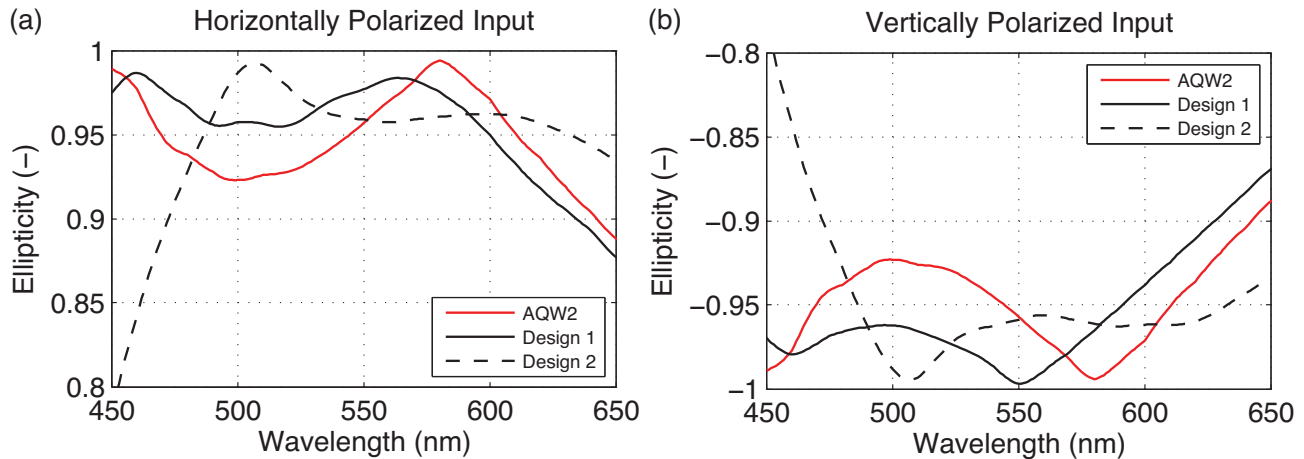


Figure 5. Measured ellipticity values for two-twist samples and comparison commercial sample for (a) horizontally polarized, and (b) vertically polarized inputs respectively.

5. EXPERIMENTAL RESULTS

Using the process described in the last section, we have successfully fabricated several broadband QWPs using different combinations of two LC twist layers. Here we discuss the performance of representative samples where the target was to achieve the design parameters in Table 1. To compare our results, we used a commercial product that was designed using one of the conventional approaches discussed in the beginning. This product, AQW2 (Colorlink Inc., Japan) is manufactured by arranging several stacks of stretched polymer films designed to achieve linear to circular polarization conversion (and vice versa) in the visible range, and represents a good baseline for our samples.

5.1 Achromatic QWPs using two twist layers

In Fig. 5, we show the ellipticity data measured for a couple of our representative two-twist samples, and the comparative QWP: AQW2. The naming scheme is consistent with the respective design parameters in Table 1. We measured ellipticity for both horizontally and vertically linearly polarized inputs. This data was initially calculated by measuring the stokes parameter S_3 using well documented techniques.¹⁵ These measurements have also been confirmed by an independent source (Colorlink Inc., Japan) using a commercial measurement tool, Axoscan. First, it is easy to see for both of the polarizations, both the two-twist samples achieve broadband QWP operation with $|e| \approx 1$ over the entire visible range. Second, this performance matches, and in one case even exceeds, the performance of AQW2. This is truly remarkable considering the simplicity of the fabrication process highlighted earlier. In order to compare the net performance of these elements, an average ellipticity $\langle e \rangle$ was calculated using the measured data. These values have been summarized in Table 3. Here we can once again see evidence of the broadband performance, that is similar to the calculated values in Table 2. The differences in broadband performance between the measured values in Fig. 5 and the calculated values in Fig. 3 is purely related to tolerances in the fabrication process. The average ellipticity can be improved further by fine-tuning the processing parameters.

Fig. 6 describes a different approach to characterize the twist waveplates. When the waveplate is arranged with the second twist layer facing the input, it can effectively convert circularly polarized light back into a corresponding linear polarization. Qualitatively we can observe this using the setup shown in part (a). We use AQW2 to create the circular polarization from a linear polarizer as shown. The output from the two-twist waveplate is then observed through an analyzer set orthogonal to the input polarizer. In part (a), the AQW2 film when viewed through crossed polarizers appears bright since half of the circularly polarized light leaks through. The two-twist QWP is placed on top of the AQW2 film, and then viewed through the analyzer in part (c). Here we can see that in the region of the waveplate almost all of the light is blocked by the analyzer indicating that almost all of the light has been converted back to horizontally polarized light by the twist waveplate.

DESIGN TYPE	Horizontally Polarized Input	Vertically Polarized Input
Commercial Product: AQW2	0.9473	-0.9473
Two-twist Design 1	0.9537	-0.9533
Two-twist Design 2	0.9428	-0.9431

Table 3. Comparison of average ellipticity (e) measured for orthogonal linear polarizations calculated over the visible range of 450-650 nm.

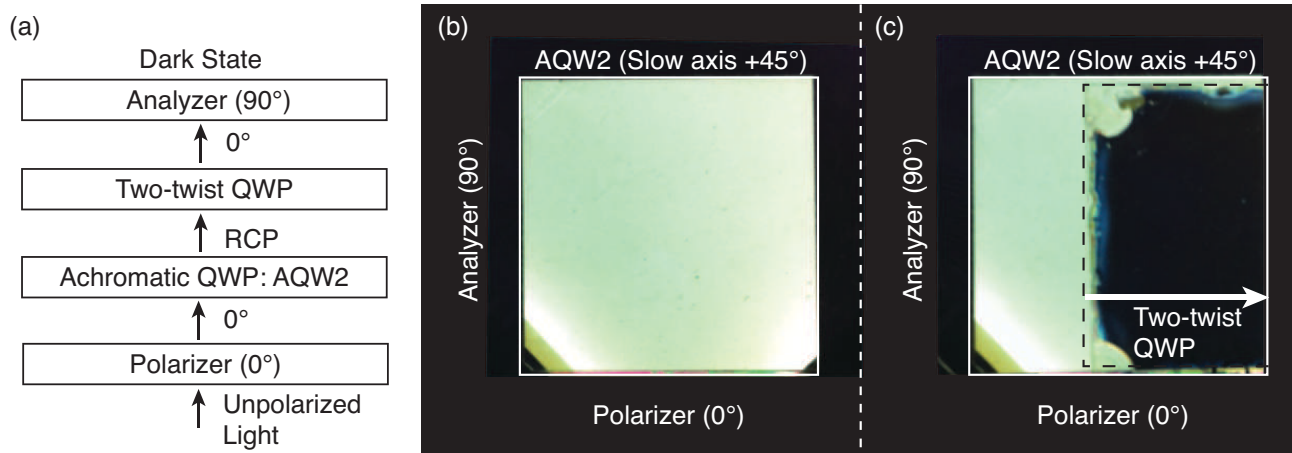


Figure 6. (a) Measurement setup to evaluate circular to linear conversion of two-twist QWP. Crossed polarizer images of (a) commercial broadband QWP: AQW2, and (b) stack of AQW2, two-twist QWP showing good extinction by output analyzer as in part (a).

5.2 Patterned MTRs

Broadband MTRs can be easily formed as multiple (i.e., two or more) discrete domains for various applications by appropriately patterning the alignment layer. The only constraint is that the lateral dimensions of the domains are required to be much larger than the wavelength of light (and the thickness of the birefringent layer) in order to avoid diffraction. Patterned retarders such as these can provide polarization transformation with a spatial variation, and have applications in 3D LCDs, polarization imaging cameras, and other optical systems including Polarization Conversion Systems (PCS).¹⁶ In these cases, the individual domains accept polarizations of different handedness and may be used to convert them to a single global polarization, and vice versa.

An example 1D louvered waveplate is illustrated in Fig. 7, but more complicated 2D patterns can be easily created similarly. The exposure process is shown in part (a) where an LPP coated sample receives polarized light through a chrome mask. The mask has a pitch of 1 mm and a fill factor of 50%. The LPP is patterned in a two-step process where the polarizer is set to 0 and 90 respectively in neighboring domains. A translation stage is used to adjust the location of mask to block the corresponding domains in each case. The LCP coating process is identical to that used for non-patterned waveplates. Part (b) shows a sample that is analyzed through a polarizing microscope similar to Fig. 6a where a AQW2 film is inserted in the beam path. Since orthogonal exposure angles were used in the neighboring domains, the twist waveplate causes the analyzer to selectively block and transmit the corresponding linear polarization in each domain. There seems to be no observable scattering due to defect lines at the boundary indicating good alignment for most of the area. Similar techniques could be used to achieve more complicated patterns.

6. CONCLUSION

We describe a simple arrangement of twisted nematic liquid crystal layers that forms a monolithic birefringent plate that accomplishes well-controlled polarization transformation for nearly any wavelength, bandwidth, or incident angle range desired, including, but not limited to, broadband (i.e., achromatic) quarter-wave and half-wave retardations. Methods in the prior art using individual and multiple stacks of simple birefringent elements

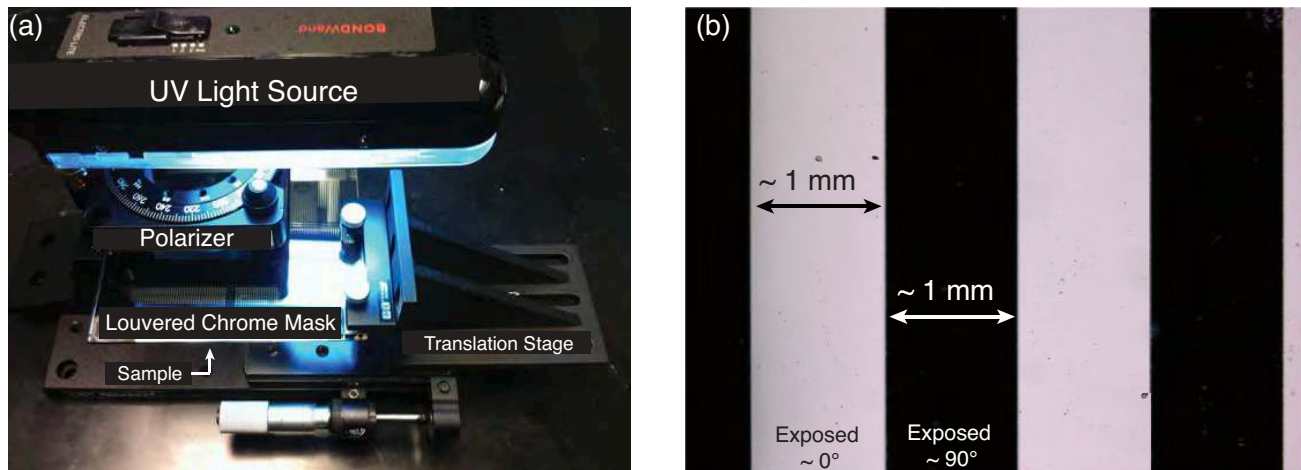


Figure 7. (a) Exposure setup to create louvered twist waveplates. (b) Polarization microscope image of louvered broadband twist QWP showing orthogonally exposed regions.

are unable to achieve the broadband polarization transformation performance desired, and/or cannot easily offer large clear apertures, small thicknesses, or acceptable cost. The twisted waveplates discussed are monolithic birefringent elements fabricated on a single substrate, that accomplish well-controlled polarization transformation. Just two twist layers achieve broadband quarter-wave retardation with excellent performance and potentially very low cost. However, the use of multiple self-aligned twist layers presents a very general retarder technique, where more layers can be added to the design for better broadband control, or to target any retardation profile and not just for quarter-wave plates as described in this work.

ACKNOWLEDGMENTS

The authors acknowledge financial support from ImagineOptix Corp for this work. Additionally, we gratefully acknowledge Merck Chemicals Ltd. for access and advice on the RMS materials, and ColorLink Japan Ltd. for samples, and useful discussions.

REFERENCES

- [1] Broer, D., Lub, J., and Mol, G., "Wide-band reflective polarizers from cholesteric polymer networks with a pitch gradient," *Nature* **378**(6556), 467–469 (1995).
- [2] Yeh, P. and Gu, C., [*Optics of liquid crystal displays*], Wiley, New Jersey (2010 (second edition)).
- [3] Cescato, L., Gluch, E., and Streibl, N., "Holographic quarterwave plates," *Applied Optics* **29**(22), 3286–3290 (1990).
- [4] Samoylov, A., Samoylov, V., Vidmachenko, A., and Perekhod, A., "Achromatic and super-achromatic zero-order waveplates," *Journal Of Quantitative Spectroscopy & Radiative Transfer* **88**(1-3), 319–325 (2004).
- [5] Clarke, D., "Achromatic halfwave plates and linear polarization rotators," *Optica Acta* **14**(4), 343–350 (1967).
- [6] Schirmer, J., Kohns, P., Schmidt-Kaler, T., Yakovenko, S., Muravski, A., Dabrowski, R., Adomenas, P., and Stolarz, Z., "Achromatic phase retarders using double layer liquid crystal cells," *Proceedings of the SPIE - Liquid Crystals: Physics, Technology and Applications* **3318**, 358–363 (1998).
- [7] Pancharatnam, S., "Achromatic combinations of birefringent plates: Part 1," *Proceedings of the Indian Academy of Sciences A* **41**, 130–136 (1955).
- [8] Schadt, M. and Helfrich, W., "Voltage dependent optical activity of a twisted nematic liquid crystal," *Applied Physics Letters* **18**(4), 127–128 (1971).
- [9] Scheffer, T. and Nehring, J., "Supertwisted nematic (STN) liquid crystal displays," *Annual Review of Materials Science* **27**, 555–583 (1997).

- [10] Zhuang, Z., Kim, Y., and Patel, J., “Achromatic linear polarization rotator using twisted nematic liquid crystals,” *Applied Physics Letters* **76**(26), 3995–3997 (2000).
- [11] Lavrentovich, M., Sergan, T., and Kelly, J., “Switchable broadband achromatic half-wave plate with nematic liquid crystals,” *Optics Letters* **29**(12), 1411–1413 (2004).
- [12] Shen, S., She, J., and Tao, T., “Optimal design of achromatic true zero-order waveplates using twisted nematic liquid crystal,” *Journal of the Optical Society of America A - Optics Image Science and Vision* **22**(5), 961–965 (2005).
- [13] Oh, C. and Escuti, M. J., “Achromatic diffraction from polarization gratings with high efficiency,” *Optics Letters* **33**(20), 2287–2289 (2008).
- [14] Seo, E., Kee, H., Kim, Y., Jeong, S., Choi, H., Lee, S., Kim, J., Komanduri, R., and Escuti, M., “Achromatic diffraction from polarization gratings with high efficiency,” *SID Symposium Digest of Technical Papers* **42**(1), 540–543 (2011).
- [15] Collett, E., [*Polarized light in fiber optics*], The PolaWave Group in association with SPIE Press (2003).
- [16] Parri, O., Smith, G., Harding, R., Yoon, H., Gardiner, I., Sargent, J., and Skjonnemand, K., “Patterned Retarder Films using Reactive Mesogen Technology,” *Proceedings of SPIE - Advances in Display Technologies and E-papers and Flexible Displays* **7956**, 79560W (2011).